ScienSage

Journal of Advanced Scientific Research

Available online through https://sciensage.info

ISSN
0976-9595
Research Article

IMPEDANCE SPECTROSCOPY GENETIC PROGRAMMING (ISGP) ANALYSES SETTING PROPER WORKING CONDITIONS OF A POLYMER ELECTROLYTE MEMBRANE FUEL CELL

Nimai Bar*, Rajkamal Pandit

[1]*Department of Chemistry, Raja Narendra Lal Khan Women's College (Autonomous), Gople Palace, Paschim Medinipur, West Bengal, India*

[2]*Department of Physics, Raja Narendralal Khan Women's College (Autonomous), Gople Palace, Paschim Medinipur, West Bengal, India*

**Corresponding author: nimaibar635@gmail.com*

Received: 14-04-2023; Accepted: 24-08-2023; Published: 31-08-2023

© Creative Commons Attribution-NonCommercial-NoDerivatives 4.0 International License https://doi.org/10.55218/JASR.202314701

ABSTRACT

This study demonstrates application of Impedance Spectroscopy Genetic Program (ISGP) for the investigation of a polymer electrolyte membrane fuel cell (PEMFC). It further demonstrates the procedures to optimize the operating conditions of a single cell in a test station. To do that, the effects of temperature, hydrogen/air, and dew point temperature (DPT) on the cell were examined using an Arbin test station. ISGP followed a two-iteration procedure. First, find an out-of-range peak (at high frequencies) that corresponds to the ohmic (series) resistance of the system. Second, finding the models after subtracting the ohmic resistance from the real part of the measured spectrum. This two-step procedure allows solving a Fredholm equation of the second kind with a reasonable accuracy. The resulting peaks making the distribution function of relaxation time (DFRT) were partially assigned to different physical processes in the PEMFCs. ISGP seeks for a distribution of relaxation times that has the form of a peak or a sum of several peaks, assuming the Debye kernel, where each peak is represented by a known analytic function. As a part of the analysis, the peak areas, which correspond to the contribution of the relevant process to the total impedance, were calculated obtaining tendentious behavior depending on the changing environmental parameters. ISGP of PEMFC results in three peaks. The optimized conditions were found to be the ratio of gas flow fuel to air rate 1:7, fuel cell temperature 60°C and dew point temperature 50°C.

Keywords: Distribution function of relaxation time, proton exchange membrane fuel cell, impedance spectroscopy genetic programming, Arbin fuel cell test station.

1. INTRODUCTION

Polymer lectrolyte membrane fuel cells (PEMFC) have a great deal of potential applications due to their high power and energy densities and low operating temperature [1-9]. PEMFCs serve electrical energy generation, and power sources for transportation and find applications in the stationary and mobile phase/industry [10, 11]. Impedance study on PEMFCs is usually done on small (ca. 1-25 cm^2) devices in order to have measureable values. The performance of such devices are known to be influenced by many parameters such as the operating temperature, fuel/air temperatures, and the feeding rate of the gases [12], all of which are controlled by the test system. The studies are done on a single Membrane Electrode Assembly (MEA), which consists of five layers: two gas-diffusion layers (GDL), two supported-catalyst layers (CL), and a membrane [13].

Electrochemical impedance spectroscopy (EIS) is a powerful and non-destructive method of characterizing the electrical properties of materials and electrochemical devices. There are several analytical methods for the analysis of EIS data. The approach used herein for MEA analysis by EIS is based on finding the distribution function of relaxation times (DFRT) of the measured sample according to the formula:

$$Z(\omega) = Z(\infty) + R_{pol}\int_{-\infty}^{\infty}\frac{\gamma(\log(\tau))}{1+i\omega\tau}d(\log(\tau)) \quad (1)$$

where Z(ω) is the impedance, ω the frequency, R_{pol} the totalresistance, □ the DFRT, and τ the relaxation time [14-18]. To find the DFRT model that best fits the measured data, we analyze the data using the Impedance Spectroscopy Genetic Program (ISGP) [19, 20], which finds an *analytical form* of the DFRT. ISGP also ensures that the chosen DFRT would have a minimal number of peaks or free parameters, by using the discrepancy-complexity approach [21]. The outcome of this analysis is an analytical function of the distribution of relaxation times in the tested device, where its convolution with the Debye kernel (eq. 1), gives the best fit to the measured data. A more comprehensive explanation of the analysis is beyond the scope of this paper, but is fullypresented in the above references. It has been also demonstrated on electrochemical systems such as SOFC, cathode half cells [22] and anode half cells [23], SOFC-SOEC full cells [24], supercapacitors [25] and pseudo-supercapacitors [26]. Here we apply it to a PEMFC MEA mounted in an Arbin electrochemical test station.

2. EXPERIMENTAL

The MEA (ArbinMEA-H2-051-5L) is composed of five layers, 5 cm^2 electrode surface, NAFION 112 membrane, electrodes of carbon cloth, and double serpentine topology in anode and cathode. The Arbintest system (FCTS 50 HE) allows PEM fuel cell activation by supplying fuel (hydrogen) and oxidant (air) at varying flow rates. The system also enables the determination and monitoring of other operating parameters such as the temperature of the passing gases, the temperature of the cell itself, and the relative humidity of the gases.

Table 1: Technical specifications of the device under test

Five layer MEA with integrated GDL	
Membrane Area (cm^2)	5
Active Area (cm^2)	4.84
Type	Nafion 212
Catalyst	
Anode Catalyst	60 wt % Pt on Vulcan (Carbon)
Anode Loading(mg/cm^2)	0.5
Cathode Catalyst	60 wt % Pt on Vulcan (Carbon)
Cathode Loading (mg/cm^2)	0.5
Gas Diffusion Layer	
Fiber Type	Cloth
Thickness (μ)	410

2.1. Electrochemical Impedance Spectroscopy (EIS)

Impedance data were recorded using a Gamry Reference 3000 system, with a frequency sweep from 0.1 Hz to 1 MHz and an ac signal of 50 mV in hybrid mode. The experimental impedance data consist an inductance at high frequencies and a positive imaginary part at low frequencies. These parts were removed before the ISGP analysis (high frequency limit was typically set at 10 kHz).Two impedance data sets per run were loaded (f, Z' and -Z") and checked by Kramers-Kronig transformation for validation. We use two sets of data per run to avoid over fitting. This is done by finding the parameters of the DFRT using one set, but assessing the discrepancy using a linear combination of the two sets [20]. Each pair of loaded data sets were run three times up to 300 generations, selecting pseudo-delta, hyperbolic secant, Gaussian, Lorentzian and out-of-range pseudo-delta as possible peaks from the program's library. The out-of-range peak was selected to estimate the contribution of ohmic resistance.

ISGP results in three peaks, one of which is due to ohmic resistance and the other two due to cathode reaction. To improve accuracy, the ohmic resistance was subtracted from the experimental data (real part) and the subtracted data was run once again. The location (time constant) of the peaks is its characteristic relaxation time while the area is related to the (effective) resistance or active part [17].

3. RESULTS AND DISCUSSION

3.1. Finding the optimal Fuel Cell Temperature

The PEMFC operating temperatures were varied from 40°C to 80°C at 10°C increasing intervals. During the measurement, other parameters like gas flow rate, dew point temperature of both fuel and air remain constant. After subtracting the ohmic resistance, ISGP shows two peaks that are assigned here as HF (low log(τ), most probably related to charge transfer) and LF (high log(τ), most probably related to mass transfer). Both the relaxation time (i.e., the central position of the peaks) and the effective resistance are functions of the fuel cell temperature. The total resistance can be expressed as a sum of the contributions from contact resistance and ohmic resistance of the cell components including membrane, catalyst layer, and gas diffusion layer. The biggest contributor is the membrane resistance, which is subtracted before the calculations here. The other major effects of temperature are to change the reaction kinetics

of the oxygen reduction reaction (ORR) in the fuel cell and to increase the mass transfer [27-29].

Fig.1 shows a shallow minimum resistance at 60°C of the PEMFC. The HF contribution is relatively small with trend (except the unexplained deviation at 40°C) of decreasing impedance with increasing temperature. The larger LF contribution is responsible for the above-mentioned shallow minimum. This suggests that the LF peak has some non-negligible contribution from the membrane. Increasing the cell temperature should decrease the mass transfer limitations, whereas the constant GST combined with increasing cell temperature reduces the relative humidity and can influence the protonic mobility in the membrane [30, 31]. The impedance of the full fuel cell at low frequencies where the electrode impedance prevail, almost equals the cathode impedance due to the fast hydrogen oxidation reaction. The charge-transfer resistance (R_{ct}) is the sum of both the anode and cathode [32-36].

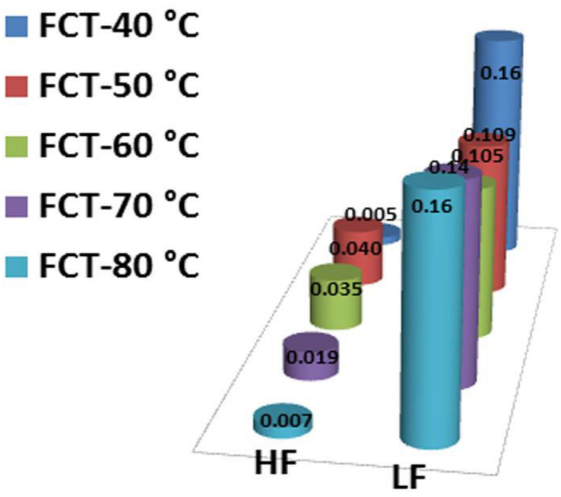

Resistance values were calculated by the peak area multiplied by the normalization factor (ideally, the polarization resistance) $A \cdot R_p$.

Fig. 1: Calculated resistance of each peak in the DFRT of PEMFC operated at different fuel cell temperatures (FCT)

Fig.2 is the DFRT plot of PEMFC at different fuel cell temperatures. With increasing temperature from 40°C to 60°C the effective resistance decrease while the relaxation times remain roughly constant. This implies that the effective capacitance (the reactive part) is increased with temperature. At high temperatures, above 60°C, the resistance increases due to the reduction of water content (Fig.1). For further measurements of dew point temperature and air/fuel flow rate effect, the fuel cell temperature was fixed at its optimal temperature, namely, at 60°C.

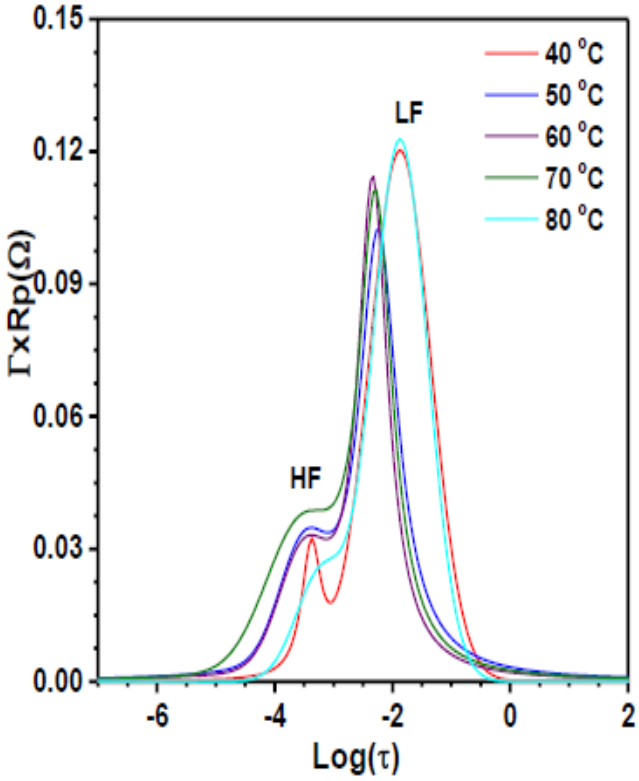

Fig. 2: Distribution function of relaxation time (Γ *vs* log(τ)) plot for the fuel cell operating at different temperatures

3.2. Effect of gas flow rate

The hydrogen flow was changed while the flow of air remained constant and the air flow rate was changed while the hydrogen flow remained constant. Three ratios (1:3, 1:5, and 1:7) were tested. The measurements are performed for a cell temperature of 60°C, dew point temperature of 50°C, and gas supply temperature (GST) of 50°C after an hour of stabilization. As seen in Fig.3, the most stable voltage (standard deviation of 1.44%) was obtained for the largest (1:7) air flow. In addition, the voltage stability was examined for different flow rates while the ratio between hydrogen and air remained constant. Due to the limitations of the Arbin test station and the hydrogen generator, we could not use a higher ratio than 1:7.

From Fig. 4, we see that the low air flow rate makes it hard to separate the two contributions to the impedance due to the poor signal to noise ratio. At low flow rate,

the ISGP results in a single broad peak. At higher flow rates, the peaks are separated due to low noise at higher flow rate. At high flow rate, the mass transfer resistance decreases compared to low rates.

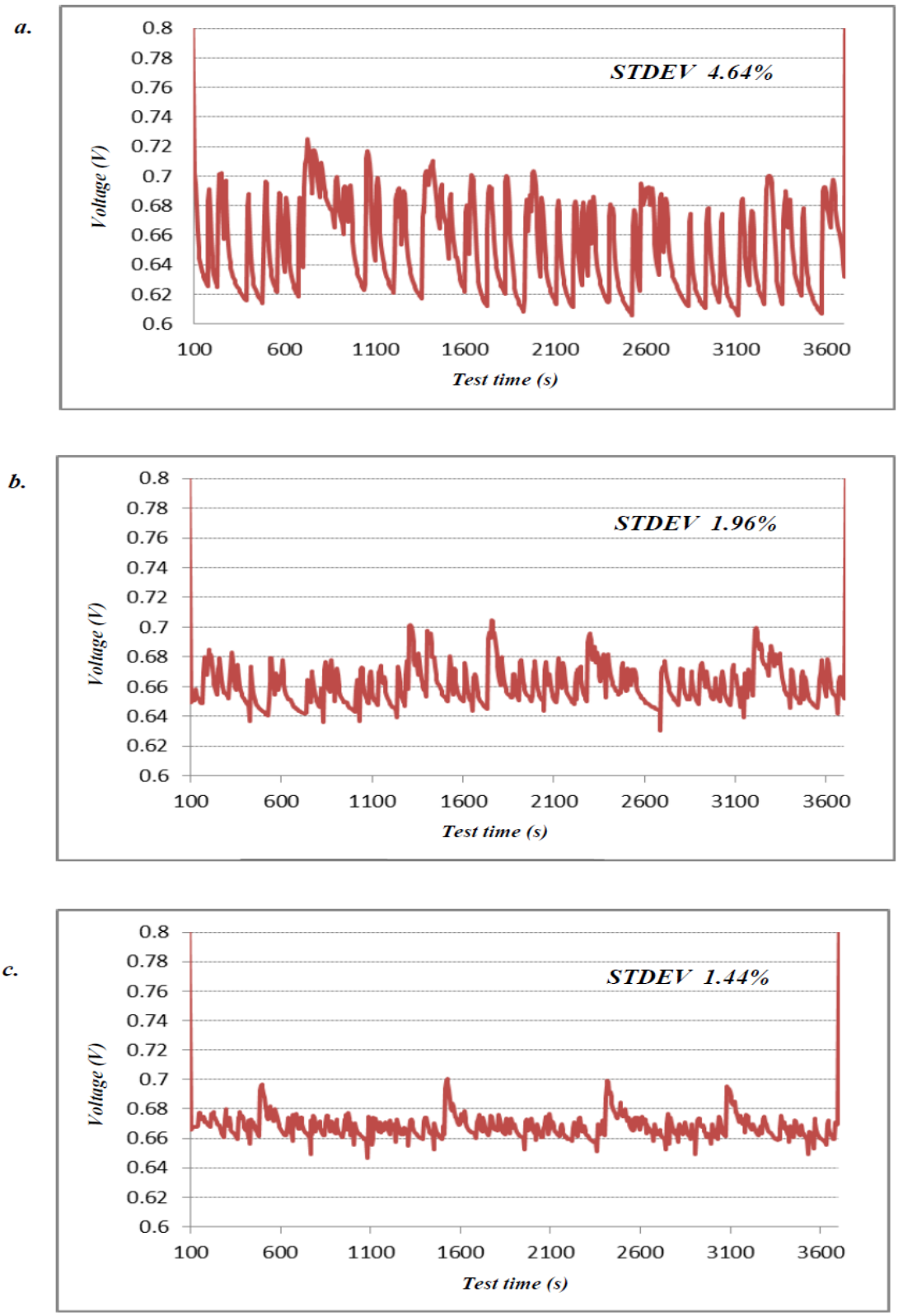

Fig. 3: voltage *vs.* time (V vs t) plots with different ratios between hydrogen flow and air flow (slpm): (a) 0.3:0.9, (b) 0.3:1.5 and (c) 0.3:2.1

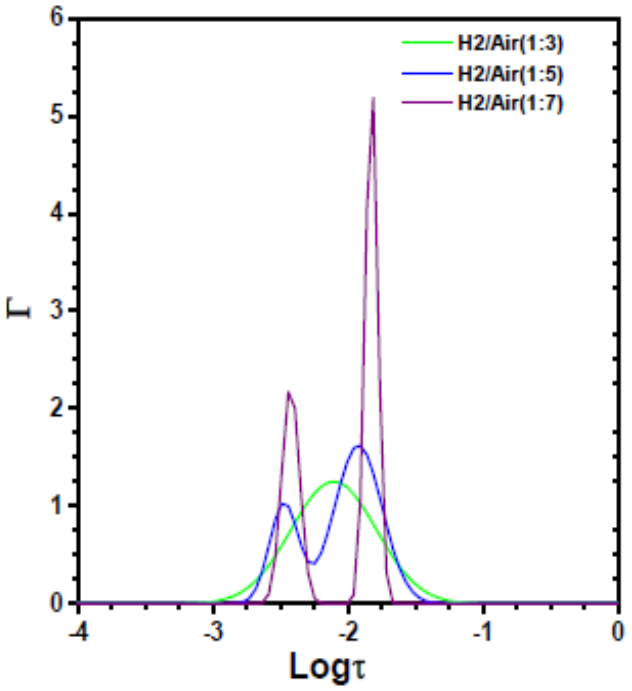

Fig. 4: distribution function of relaxation time plot obtained from PEMFC with different ratios between hydrogen flow and air flow: 0.3:0.9, 0.3:1.5, and 0.3:2.1

3.3. Effect of (fuel & air) dew point temperature

The dew point temperatures of fuel and air varied from 40°C to 80°C at 10°C increasing interval. Fig. 5(a) &(b) show the Nyquist plot of the PEFMC at different dew point temperatures after subtracting the contribution of ohmic resistance. Warburg impedance is observed at low frequency due to oxygen diffusion [37-40]. The resistance plots are given in Fig.6(a) and Fig.6(b). With increasing dew point temperatures of air and fuel observed that LF resistance does not change significantly. The dew point temperatures of fuel and air at 50°C and 60°C results slightly low mass transfer resistance compared to lower and higher dew point temperature of both air and fuel. The charge transfer resistance does change significantly with increasing dew point temperature. The attempts were to find the effect of dew point temperature on the PEMFC. The results of the dew point temperature changes are not in trend. This is due to some contributions of nafion membrane. At 50°C dew point temperatures of air and fuel slightly low mass transfer resistance. So, the dew point temperature of air and fuel were set 50°C for the optimization of other physical effect measurments.

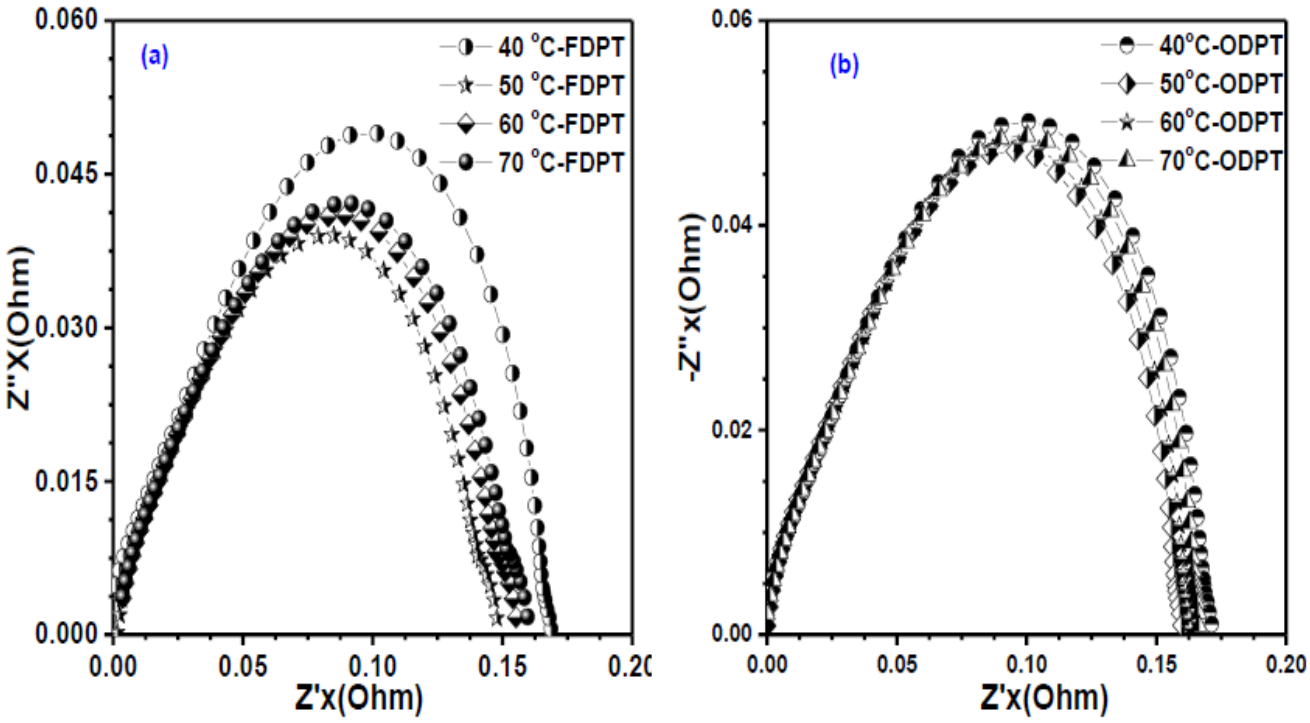

Fig. 5: (a&b): Stretched Nyquist plots (not in scale) for the polymer electrolytes membrane fuel cell at various dew point temperatures of fuel (FDPT) and air (ODPT), after subtraction of ohmic resistance

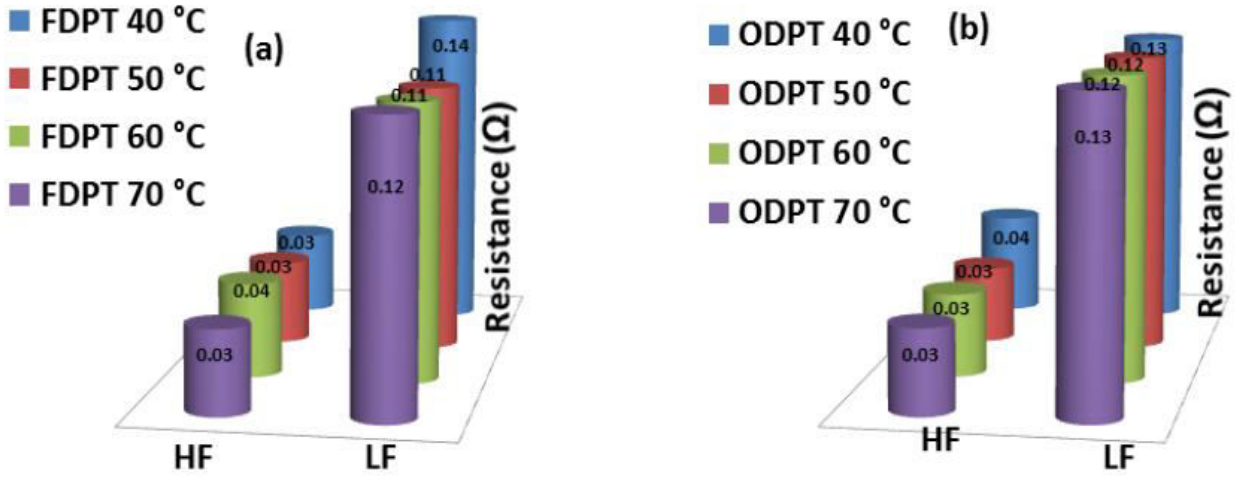

Fig. 6: Resistances of the two peaks comprising the DFRT at different dew point temperatures:(a) fuel (humidified H_2). (b) humidified air

4. CONCLUSIONS

The main objective of this work was to set the proper working conditions of a test station for EIS investigations of PEMFC. This was done by implementing ISGP, an advanced analysis method for impedance measurements. Indeed, we managed to model a polymer electrolyte fuel cell through DFRT and to examine the effects of different experimental conditions on the cell function using ISGP. Following the implementation of the fuel cell test station and its running, a series of EIS measurements at various conditions was performed, and the results were analyzed by ISGP. Most of the obtained models, regardless of the working parameters, consist of three peaks; two within the measured bandwidth and one out of it. The tendentious behavior of the peaks in the models, depending on the change in the experimental parameters, has been analyzed to assist in the processes of identifying what they represent. The out-of range peak (low logτ\high frequency) represents the contribution of ohmic resistance which arise from the polymer electrolyte membrane. This peak was subtracted for the second iteration of ISGP analysis and can be further studied by experiments consisting the change of the humidity in both sides separately. The other two peaks are related mainly to the cathode, arising from phenomena such as oxygen diffusion within the catalyst layer and charge transport limitations. The optimized conditions were found to be: ratio of gas flow fuel to air rate 1:7, fuel cell temperature 60°C, and dew point temperature 50°C.

5. ANKNOWLEDGEMENT

Nimai Bar wish to acknowledge the DST-SERB for financial support provided for project number EEQ/2022/00921.

Conflict of interest

None declared

Source of funding

None declared

6. REFERENCES

1. Larminie J, Dicks A, Fuel Cell Systems Explained, 2nd Ed., Wiley, West Sussex, Great Britain, 2003, p. 67.
2. Barbir F, PEM Fuel Cells: Theory and Practice, Elsevier, Burlington, MS, USA, 2005, p. 12.
3. Mench MM, Fuel Cell Engines, Wiley & Sons, Hoboken, NJ, USA, 2008, p. 17.
4. Doyle M, Choi SK, Proulx G. *J. Electrochem. Soc*, 2000; **147:**34.
5. Kerres J, Cui W, Disson R, Neubrand W, *J. Membr. Sci,* 1998; **139**:211.
6. Brack HP, Bu¨chi FN, Huslage J, Rota M, Scherer GG, *ACS Symp. Ser,* 1999; **744**:174.
7. Lehtinen T, Sundholm G, Holmberg S, Sundholm F, Bjo¨rnbom P, Bursell M. *Electrochim. Acta,* 1998; **43:**1881.
8. Kreuer KD, Fuchs A, Ise M, Spaeth M, Maier J. *Electrochim. Acta,* 1998; **43**:1281.
9. Paddison SJ, Paul R, Zawodzinski TA. *J. Electrochem. Soc*, 2000; **147**:617.

10. Lemons RA, *J. Power Sources,* 1990; **29**:251.
11. Wang Y, Chen KS, Mishler J, Cho SC, Adroher XC. *Applied Energy,* 2011; **88**:981.
12. Tohidi M, Mansouri SH, Amiri H. *International journal of hydrogen energy,* 2010; **35**:9338.
13. Park S, Lee JW. *International journal of hydrogen energy,* 2012; **37**:5850.
14. Scichlein H, Müller AC, Voigts M, Krügel A, Ivers-Tiffée E. *Journal of Applied Electrochemistry*, 2002; **32**:875.
15. Banys J, Lapinskas S, Kajokas A, *Phys. Rev. B*, 2002; **66**: No.144113.
16. Boukamp BA. *Electrochimica Acta*, 2015; **154**:35.
17. Hershkovitz S, Tsur Y, Baltianski S. *Solid State Ionics*, 2011; **188**:104.
18. Travassos MA, Lopes VV, Silva RA, Novais AQ, Rangel CM. *International Journal of Hydrogen Energy,* 2013; **38**:7684.
19. Hershkovitz S, Tomer S, Baltianski S, Tsur Y. *ECS Trans,* 2011; **33:**67.
20. Tesler AB, Lewin DR, Baltianski S, Tsur Y. *J. Electroceram*, 2010; **24**:245.
21. Baltianski S, Tsur Y. J. Electroceram, 2003; 10: 89.
22. Hershkovitz S, Baltianski S, Tsur Y. *Fuel Cells*, 2012; **12**:77.
23. Tomer S, Hershkovitz S, Baltianski S, Tsur Y. *Energy Technology*, 2013; **1**:25.
24. Drach Z, Hershkovitz S, Ferrero D, Leone P, Lanzini A, Santarelli M, Tsur Y. *Solid State Ionics*, 2015; **288**:307.
25. Oz A, Hershkovitz S, Belman N, Tal-Gutelmacher E, Tsur Y. *Solid State Ionics*,2016; **288**:311.
26. Borenstein A, Hershkovitz S, Oz A, Luski S, Tsur Y, Aurbach D. *J. Phys. Chem*. C,2015; **119**:12165.
27. Yan X, Hou M, Sun L, Liang D, Shen ., Xu H, Ming P, Yi B. *International journal of hydrogen energy*,2007; **32**:4358.
28. Hsieh SS, Yang S-H, Feng C-L. *J. Power. Sources*, 2006; **162:**262.
29. Asghari S, Mokmeli A, Samavati M. *International journal of hydrogen energy*, 2010; **35**:9283.
30. Kreuer KD. *Journal of Membrane Science*, 2001; **185**:29.
31. RikuKawa M, Sanui K. *Prog. Polym. Sci*. 2000; **25**:1463.
32. Malevich D, Halliop E, Peppely BA, Pharoah JG, Karan K. *Journal of The Electrochemical Society*, 2009; **156**:B216.
33. Wagner N. *Journal of Applied Electrochemistry,* 2002; **32**:859.
34. Tatiana JPF, Gonzalez ER. *Journal of. Electroanalytical Chemistry,* 2001; **503**:57.
35. Andreaus B, MacEvoye AJ, Scherer GG. *Electrochimica Acta*, 2002; **47:**2223.
36. Cho EA, Jeon U-S, Ha HY, Hong S-A, Oh I-H, *Journal of Power Sources*, 2004; **125**:178.
37. Hana M, Xua JH, Chana SH, Jiang SP. *Electrochimica Acta*, 2008; **53**:5361.
38. Singh RK, Devivaraprasad R, Kar T, Chakroborty A, Neergat M. *Journal of The Electrochemical Society*, 2015; **162**:F489.
39. Prasanna M, Ha HY, Cho EA, Hong S-A, Oh I-H. *J. Power Sources,* 2004; **131**:147.
40. Bultel Y, Wiezell K, Jaouen F, Ozil P, Lindbergh G. *Electrochimica Acta,* 2005; **51**:474.